Geophys. J. Int. (2006) **165,** 957–968 doi: 10.1111/j.1365-246X.2006.02968.x

Seismic attenuation due to wave-induced fluid flow in a porous rock with spherical heterogeneities

R. Ciz,[1] B. Gurevich[1,2] and M. Markov[3]

[1] *CSIRO Petroleum, ARRC,* 26 *Dick Perry Ave, Tech. Park, Kensington, Perth, Western Australia* 6151, *Australia. E-mail: radim.ciz@csiro.au*
[2] *Curtin University of Technology, Department of Exploration Geophysics, GPO Box* U1987, *Perth, Western Australia* 6845, *Australia*
[3] *Instituto Mexicano del Petroleo, Eje Central Lazaro Cardenas* 152, CP 07730, *Mexico*

Accepted 2006 February 22. Received 2006 February 21; in original form 2005 May 28

SUMMARY

Most natural porous rocks have heterogeneities at nearly all scales. Heterogeneities of mesoscopic scale—that is, much larger than the pore size but much smaller than wavelength—can cause significant attenuation and dispersion of elastic waves due to wave-induced flow between more compliant and less compliant areas. Analysis of this phenomenon for a saturated porous medium with a small volume concentration of randomly distributed spherical inclusions is performed using Waterman-Truell multiple scattering theorem, which relates attenuation and dispersion to the amplitude of the wavefield scattered by a single inclusion. This scattering amplitude is computed using recently published asymptotic analytical expressions and numerical results for elastic wave scattering by a single mesoscopic poroelastic sphere in a porous medium.

This analysis reveals that attenuation and dispersion exhibit a typical relaxation-type behaviour with the maximum attenuation and dispersion corresponding to a frequency where fluid diffusion length (or Biot's slow wavelength) is of the order of the inclusion diameter. In the limit of low volume concentration of inclusions the effective velocity is asymptotically consistent with the Gassmann theory in the low-frequency limit, and with the solution for an elastic medium with equivalent elastic inclusions (no-flow solution) in the low-frequency limit. Attenuation (expressed through inverse quality factor $1/Q$) scales with frequency ω in the low-frequency limit and with $\omega^{-1/2}$ in the high-frequency limit. These asymptotes are consistent with recent results on attenuation in a medium with a periodic distribution of poroelastic inclusions, and in continuous random porous media.

Key words: attenuation, Biot's slow wave, poroelastic media, scattering, wave propagation.

1 INTRODUCTION

Seismic attenuation and dispersion are wavefield characteristics that can provide important information about the structure and composition of a medium. It is well known that Biot's (1962) theory of elastic wave propagation in homogeneous porous media underestimates the observed attenuation and dispersion by at least one order of magnitude. One possible cause of the larger than predicted attenuation is associated with the presence of spatial heterogeneities (Pride *et al.* 2003). When a porous medium contains regions of variable compliance, the passing compressional wave can cause pore fluid to flow from more compliant to less compliant areas and vice versa. Analysis of this phenomenon requires a theoretical model of wave propagation in an inhomogeneous porous medium.

Theoretical studies of elastic wave attenuation and dispersion in saturated porous media due to the presence of small-scale heterogeneities were initiated in the 1970s, when J.E. White and his colleagues introduced two theoretical models of this phenomenon. They developed a 1-D model of a finely layered porous medium (White *et al.* 1976) consisting of alternating layers of gas and liquid saturation, and a 3-D model of an array of spherical gas patches embedded in a homogeneous liquid-saturated porous background (White 1975). The results of these studies were later rederived using Biot's (1962) theory of poroelasticity by Norris (1993) and Dutta & Ode (1979a,b), respectively.

Common to all of the above formulations, was the fact that, they modelled regular (periodic) heterogeneities of the porous medium. For 1-D media, this was recognized as a limitation by Lopatnikov & Gurevich (1986), who developed a theoretical model for elastic wave attenuation and dispersion in randomly layered porous materials (Gurevich & Lopatnikov 1995). They showed that behaviour of the frequency dependent attenuation and dispersion is quite different for random and periodic layering.

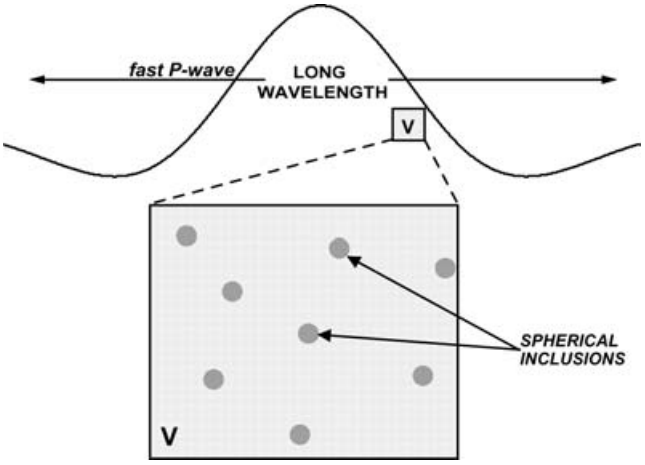

Figure 1. Configuration of the model representing randomly distributed inclusions in the poroelastic background medium. The wavelength of incident wave is much longer than the size of inclusions, where inclusion is much larger than individual pores (modified from Pride & Berryman 2003).

For 3-D heterogeneities, Johnson (2001) developed an approximate theory, which generalizes the results of White (1975) to a periodic ensemble of fluid patches of arbitrary shape. Recently, a more general model was proposed by Pride & Berryman (2003) and Pride *et al.* (2004), which allows for an ensemble of inclusions with contrast in any material properties (the so-called double-porosity, dual-permeability medium). However, common to all the 3-D models proposed so far is the fact that, they are limited to regular spatial configurations of heterogeneities. An exception is the work of Gurevich *et al.* (1998) who analysed the propagation of an elastic wave in a porous medium with randomly distributed spheriodal inclusions. However, this particular work was based on the solution of a scattering problem using the Born approximation. Thus, it was limited to small contrasts in material properties between the inclusion and background medium—a situation of limited interest for most applications.

This mechanism of attenuation for the continuous random inhomogeneities has been analysed by Muller & Gurevich (2005). In this paper we analyse the effect of randomly distributed spherical inclusions of another porous material. The size of the inclusions is assumed to be mesoscopic, that is, much larger than an individual pore size, but much smaller than the wavelength of a fast compressional and shear wave. The problem is solved by firstly considering the interaction of a plane elastic *P* wave with a single spherical inclusion, then by applying an approximate theory of multiple scattering (Waterman & Truell 1961), the effect of an ensemble of inclusions is estimated. The situation analysed is shown in Fig. 1.

2 APPROACH

2.1 Scattered amplitude from a single spherical inclusion

Following Berryman (1985), we consider the problem of scattering of an elastic wave in a poroelastic medium (called background medium) by a spherical inclusion of another poroelastic material. Specifically, we consider a fast compressional plain-wave incident on a spherical inclusion. When this incident wave interacts with the inclusion, it produces fast compressional, slow compressional and shear waves in the background medium (called scattered or reflected waves), and waves of the same three kinds inside the inclusion (called refracted waves). We assume that the size of the inclusion is much smaller than the fast compressional wave, but is not restricted with respect to the wavelength of the Biot's slow wave. This is the main difference from Berryman's (1985) long-wavelength solution, which assumes the size of the inclusion to be much smaller than both wavelength of fast compressional wave and wavelength of Biot's slow wave. The dynamic behaviour of both materials is described by Biot's (1962) equations of poroelasticity. We consider a porous background medium with the uniformly distributed porosity ϕ whose pores are filled with a viscous fluid with bulk modulus K_f, density ρ_f and viscosity η. The grains of the solid are characterized by bulk modulus K_g, shear modulus μ_g and density ρ_g. The solid skeleton formed from grains is characterized by bulk modulus K_0, shear modulus μ_0, density ρ_0 and permeability κ. The inclusion parameters are denoted by the same symbols with prime. We also assume that the frequencies are lower than Biot's characteristic frequency so that the undrained bulk moduli of each porous material (background or inclusion) saturated by a compressible fluid are described by Gassmann's (1951) equation

$$K = K_0 + \sigma C, \tag{1}$$

where

$$\sigma = 1 - \frac{K_0}{K_g}, \tag{2}$$

$$C = \sigma M, \tag{3}$$

and

$$M^{-1} = \left[\frac{\sigma - \phi}{K_g} + \frac{\phi}{K_f}\right]. \tag{4}$$

Alternatively, Gassmann's eq. (1) can be rewritten for the undrained *P*-wave modulus $H = K + 4\mu/3$:

$$H = L + \sigma C, \tag{5}$$

where $L = K_0 + 4\mu/3$ is *P*-wave modulus for the dry frame.

Several researchers have studied the problem of scattering in the elastic and poroelastic media (Yamakawa 1962; Ying & Truell 1956; Gubernatis *et al.* 1977; Krutin *et al.* 1984; Korneev & Johnson 1993a,b; Zimmerman & Stern 1993). The general solution of a the problem of scattering of a harmonic plane wave by a spherical inclusion in terms of spherical Bessel functions and Legendre polynomials is given by Yamakawa (1962). This solution was extended by Berryman (1985) to poroeleastic media. This solution must obey the boundary conditions (Deresiewicz & Skalak 1963) on poroleastic interface, that is, continuity of normal and tangential component of stresses, continuity of solid and relative fluid displacements and continuity of the pore fluid pressure. The detailed analysis of this problem within the low-frequency regime of Biot's theory is given by Ciz & Gurevich (2005) who derived simple expressions for the amplitude of scattered Biot's slow wave. Here we extend this analysis and derive the fast *P*-wave amplitude scattered by the spherical poroelastic inclusion embedded in the poroelastic background medium. The expressions for the fast *P*-wave amplitude will be used in the next section for computing the attenuation and dispersion.

According to Ciz & Gurevich (2005), the solution for the radial component of the displacement of the scattered wave into the background medium in the far field is

$$u_{1r} = -\sum_{n=0}^{\infty}(-i)^n\left[\frac{B_n^+}{k_+^2}\frac{e^{ik_+r}}{r} - \frac{B_n^-}{k_-^2}\frac{e^{ik_-r}}{r}\right]P_n(\cos\theta), \tag{6}$$

where k_+ is the wavenumber of the fast compressional wave, k_- represents the wave number of the slow compressional wave and $P_n(\cos\theta)$ is the Legendre polynomial of the order n. The coefficients for the scattered fast wave are B_n^+ for $n = 0, 1, 2$; for the scattered slow wave, they are B_n^- for $n = 0, 1, 2$.

Since we assumed from the outset that our inclusion is small compared to the wavelength of the fast wave, we can regard eq. (6) as a series in small parameter k_+a. The terms with $n \geq 3$ for the scattered fast wave are of the order $(k_+a)^5$ and are, therefore, negligible (Yamakawa 1962). Furthermore, it has been shown by Ciz & Gurevich (2005) that the contributions from the terms B_1^- and B_n^- for $n \geq 3$ are proportional to k_+a, and these terms are small compared to B_0^- and B_2^-. Thus, the wavefield of the scattered slow wave is given by two terms of the orders 0 and 2. The scattering amplitude for $n = 0$ is given by the expression (Ciz & Gurevich 2005):

$$B_0^- = \frac{\xi_-}{h_1^{(1)}(\xi_-)}\frac{CA_0}{\left[N'\frac{j_0(\xi'_-)}{j_1(\xi'_-)}\xi'_- - N\frac{h_0^{(1)}(\xi_-)}{h_1^{(1)}(\xi_-)}\xi_- + 4\frac{C'^2}{H'H''}(\mu - \mu')\right]}\left(\frac{C}{H} - \frac{C'}{H''}\right), \tag{7}$$

where prime denotes parameters inside the inclusion, A_0 is the amplitude of the incident *P* wave, $h_1^{(1)}$, $h_0^{(1)}$, j_0, j_1 are spherical Bessel functions of the orders 0 and 1, $H'' = K' + 4\mu/3$, $\xi'_- = k'_-a$, $\xi_- = k_-a$, $N = ML/H$ and $N' = M'L'/H'$. The full expression for $n = 2$ (Ciz & Gurevich 2005) is very complicated, but can be simplified assuming that the amplitude of the scattered fast (normal) compressional and shear waves are well approximated by the solution of the equivalent elastic problem. This assumption yields a simple approximation for the amplitude of the scattered slow wave, which is quite accurate for a wide range of material properties and is sufficient for the analysis of the scattering amplitude as a function of frequency. This expression reads

$$B_2^- = \frac{\left(\frac{j_1(\xi'_-)}{j_2(\xi'_-)} - \frac{3}{\xi'_-}\left(1 - \frac{N'\xi'^2_-}{N\xi^2}\right)\right)X_2^E}{h_2^{(1)}(\xi_-)\xi'_-N'\frac{L}{\sigma}\left[\frac{1}{N'\xi'_-}\left(\frac{j_1(\xi'_-)}{j_2(\xi'_-)} - \frac{3}{\xi'_-}\right) - \frac{1}{N\xi_-}\left(\frac{h_1^{(1)}(\xi_-)}{h_2^{(1)}(\xi_-)} - \frac{3}{\xi_-}\right)\right]}, \tag{8}$$

with

$$X_2^E = \frac{-20A_0C\mu(\mu' - \mu)}{(16\mu\mu' + 6\lambda\mu' + 14\mu^2 + 9\lambda\mu)}, \tag{9}$$

where $h_1^{(1)}, h_2^{(1)}, j_1, j_2$ define spherical Bessel functions of orders 1 and 2, λ, λ' represent fluid-saturated Lamé coefficients in the background and inclusion. In the long-wavelength limit eq. (7) reduces to the long-wavelength approximation of B_0^- derived by Berryman (1985). In the low-contrast limit eqs (7) and (8) reduce to the solution derived by Gurevich *et al.* (1998) using the Born approximation. In the low-frequency limit, Biot's slow wave amplitude scales with $\omega^{3/2}$ while for inclusions larger than the wavelength of Biot's slow wave, the scattering amplitude is proportional to $\omega^{1/2}$.

To derive the fast compressional wave coefficients of the scattered wave amplitude required for the attenuation analysis, we use the same concept. We solve the 4×4 system of boundary conditions for the coefficient of order $n = 0$ at the inclusion surface and the 6×6 system of boundary conditions for $n = 2$. These solutions give the expressions for the fast compressional wave coefficients B_0^+ and B_2^+:

$$B_0^+ = \frac{i\xi_+^3A_0(K - K')}{3H''} - \frac{i\xi_+^3h_1^{(1)}(\xi_-)}{\xi_-}\left(\frac{HC'}{H''C} - 1\right)B_0^-, \tag{10}$$

$$B_2^+ = \frac{4}{3}\frac{i\xi_+^3\mu(\mu'-\mu)\left(5A_0\xi_- + 3h_1^{(1)}(\xi_-)B_2^-\right)}{(16\mu\mu' + 6\lambda\mu' + 14\mu^2 + 9\lambda\mu)\xi_-}, \tag{11}$$

where $K = K_0 + \sigma C$ and $K' = K_0' + \sigma' C'$ are fluid-saturated (undrained) bulk moduli of the background and inclusion, respectively. Provided the coefficient B_1^- is small, the coefficient B_1^+ can be approximated by the effective elastic solution given by Yamakawa (1962). In the long-wavelength limit the coefficient B_0^+ from expression (10) reverts to the long-wavelength approximation derived by Berryman (1985):

$$\hat{B}_0^+ = -\frac{i\xi_+^3 A_0}{3}\frac{K_0' - K_0 + C(\sigma' - \sigma)}{\left(K_0' + \frac{4}{3}\mu\right)} + \frac{\xi_+^3}{\xi_-^3}\hat{B}_0^-, \tag{12}$$

where

$$\hat{B}_0^- = \frac{i\xi_-^3 C A_0}{3M'H}\frac{\left(CH'' - C'H\right)}{\left(K_0' + \frac{4}{3}\mu\right)}. \tag{13}$$

For completeness we also derive the long-wavelength limit for the scattered coefficient B_2^+ (eq. 11), thus the approximate coefficient $\hat{B}_2^+$ reads:

$$\hat{B}_2^+ = \frac{4}{3}\frac{i\xi_+^3\mu(\mu'-\mu)}{(16\mu\mu' + 6\lambda\mu' + 14\mu^2 + 9\lambda\mu)}\left(5A_0 - \frac{3i\hat{B}_2^-}{\xi_-^3}\right), \tag{14}$$

and

$$\hat{B}_2^- = -\frac{20}{3}\frac{i\xi_-^3 A_0 \sigma C\mu(\mu'-\mu)}{L(16\mu\mu' + 6\lambda\mu' + 14\mu^2 + 9\lambda\mu)}. \tag{15}$$

It is easy to check that if the fluid bulk modulus vanishes $K_f \to 0$, then $C \to 0$ so that $B_0^- \to 0$ and both eqs (12) and (14) reduce to the expressions B_0 and B_2 in elastic limit derived by (Yamakawa 1962). Derived expressions (10) and (11) are, therefore, consistent in the limits with known exact long-wavelength solution of (Berryman 1985) and with the solution for elastic wave scattering from a spherical inclusion derived by (Yamakawa 1962).

2.2 Multiple scattering formulae

The multiple scattering theorem of Waterman & Truell (1961) provides the method of computation of attenuation and dispersion of seismic waves in the medium with randomly distributed inhomogeneities. According to Waterman & Truell (1961), effective wavenumber k_{eff} may be calculated from the amplitudes of the scattered field as

$$\left(\frac{k_{\text{eff}}}{k_+}\right)^2 = \left[1 + \frac{2\pi\upsilon f(0)}{k_+^2}\right]^2 - \left[\frac{2\pi\upsilon f(\pi)}{k_+^2}\right]^2, \tag{16}$$

where $k_+ = \omega/v_+$ is the real wavenumber of fast P wave, υ is the density or number of scatterers per unit volume and $f(0)$, $f(\pi)$ are amplitudes of the wave scattered in the forward and backward direction (with respect to incident wave) by a single inclusion. For spherical inclusions the scattered amplitude can be related to the coefficients of the scattering series (6) by

$$f(0) = \frac{1}{ik_+}\sum_{n=0}^{\infty} i^n B_n^+, \tag{17}$$

and

$$f(\pi) = \frac{1}{ik_+}\sum_{n=0}^{\infty} (-i)^n B_n^+. \tag{18}$$

For sufficiently small concentration of inclusions quadratic terms in (16) can be neglected, which yields

$$k_{\text{eff}} = k_+\left[1 + \frac{4\pi\upsilon f(0)}{k_+^2}\right]^{1/2} \approx k_+\left[1 + \frac{2\pi\upsilon f(0)}{k_+^2}\right]. \tag{19}$$

The real part of eq. (19) gives the effective velocity v_{eff} in media with a low concentration of scatterers

$$\frac{1}{v_{\text{eff}}} = \frac{1}{v_+}\left[1 + \frac{2\pi\upsilon}{k_+^2}\text{Re}\{f(0)\}\right]. \tag{20}$$

The imaginary part of eq. (19) gives the dimensionless attenuation (inverse quality factor)

$$Q^{-1} = \frac{4\pi\upsilon}{k_+^2}\text{Im}\{f(0)\}. \tag{21}$$

The above expressions (20) and (21) allow us to model the dispersion and attenuation due to the scattering of a plane elastic wave by poroelastic inclusions randomly distributed throughout a poroelastic medium. In this study we investigate the special case of dispersion and attenuation using the solution for the scattering by a spherical inclusion given in the previous section.

3 RESULTS

3.1 Analytical results for attenuation

To derive an analytical expression for the attenuation we substitute the scattered amplitude for the fast compressional wave (eqs 10 and 11) into eq. (21). This yields

$$Q^{-1} = \frac{3\delta}{a^3 k_+^2} \mathrm{Im}\left\{\frac{1}{ik_+}\left(B_0^+ - B_2^+\right)\right\}, \tag{22}$$

where $\delta = \upsilon(4/3)\pi a^3$ is the fractional volume concentration of scatterers. As shown by Ciz & Gurevich (2005), the slow wave scattering coefficient of the order $n = 1$ is small and can be neglected. The imaginary part of the coefficient B_1^+ represents the negligible slow wave contribution. Substitution of the full expressions for B_0^+ (eq. 10) and B_2^+ (eq. 11) into (22) yields

$$Q^{-1} = \delta \mathrm{Im}\left\{\frac{h_1^{(1)}(\xi_-)}{\xi_-}\left(3\left(1 - \frac{HC'}{H''C}\right)B_0^- - \frac{4\mu\left(\mu' - \mu\right)B_2^-}{\left(16\mu\mu' + 6\lambda\mu' + 14\mu^2 + 9\lambda\mu\right)}\right)\right\}, \tag{23}$$

where B_0^- and B_2^- are slow wave coefficients given by eqs (7) and (8).

This is the expression for the attenuation of the elastic waves due to mesoscopic fluid flow induced at the boundary of randomly distributed poroelastic spherical inhomogeneities in poroelastic background medium.

In the special case of patchy saturation, where only the fluid properties between the inclusion and the background medium differ the second term in eq. (23) vanishes and we have

$$Q^{-1} = 3\delta \mathrm{Im}\left\{\frac{A_0(CH'' - C'H)^2}{HH''^2\left[N'\frac{j_0(\xi'_-)}{j_1(\xi'_-)}\xi'_- - N\frac{h_0^{(1)}(\xi_-)}{h_1^{(1)}(\xi_-)}\xi_-\right]}\right\}. \tag{24}$$

The eqs (23) and (24) constitute the main results of this paper. Before we plot effective attenuation in the full frequency range let us analyse the asymptotical behaviour at low and high frequencies.

In the low-frequency limit we can replace spherical Bessel functions with their approximate expressions for small arguments, that is, $|\xi_-| \ll 1$ (Abramowitz & Stegun 1965). Using these approximations in the expression (23) we can write Q^{-1} in the form

$$Q^{-1} = \frac{3}{2}\delta a^2\left(X_0\tilde{B}_0^- + 3\tilde{B}_2^+\tilde{B}_2^-\right)k_-^2 \propto \omega, \tag{25}$$

where coefficients X_0, $\tilde{B}_0^-$, $\tilde{B}_2^+$ and $\tilde{B}_2^-$ depend only on material properties and not on frequency

$$X_0 = \frac{HC'}{H''C} - 1, \tag{26}$$

$$\tilde{B}_0^- = -\frac{C^2H''}{3M'H}\frac{A_0X_0}{\left(K_0' + \frac{4}{3}\mu\right)}, \tag{27}$$

$$\tilde{B}_2^+ = \frac{4}{3}\frac{A_0\mu(\mu' - \mu)}{(16\mu\mu' + 6\lambda\mu' + 14\mu^2 + 9\lambda\mu)}, \tag{28}$$

$$\tilde{B}_2^- = -5\frac{\sigma C}{L}\tilde{B}_2^+. \tag{29}$$

In the high-frequency limit we substitute all spherical Bessel functions with their approximations for large arguments, that is, $|\xi_-| \gg 1$ (Abramowitz & Stegun 1965). This yields

$$Q^{-1} = \frac{3\delta\left(X_0\tilde{B}_0^- + 3\tilde{B}_2^+\tilde{B}_2^-\right)}{k_-a} \propto 1/\sqrt{\omega}. \tag{30}$$

The expressions (25) and (30) represent asymptotes of elastic wave attenuation in the poroelastic medium with low concentration of spherical inclusions of another porous material. The obtained high-frequency asymptote is consistent with the asymptotic behaviour of the solution of general diffusion equation at high frequencies (Muller & Gurevich 2005). Diffusive processes scale in the high-frequency limit as $1/\sqrt{\omega}$ and the Biot's slow wave is described by the diffusion equation. The high-frequency asymptote obtained in our model is also consistent with the result of Gurevich *et al.* (1998), whereas our low-frequency asymptote differs from the low-frequency solution of Gurevich *et al.* (1998). Q^{-1} at low-frequency scales with frequency as $\sqrt{\omega}$. The low-frequency asymptote obtained by Gurevich *et al.* (1998) was incorrect as they neglected near-field terms in wavefield expansion. Low-frequency asymptote derived in expression (25) shows attenuation scales with frequency as ω.

3.2 Velocity dispersion

To study the effect of dispersion of elastic waves in the model with randomly distributed spherical inclusions we substitute amplitudes [eqs(10) and (11)] into the expression for effective velocity (eq. 20). This substitution yields

$$\frac{1}{v_{\rm eff}} = \frac{1}{v_+}\left[1 + \frac{3}{2}\frac{\delta}{\xi_+^3}\mathrm{Re}\left\{-iB_0^+ + B_1^+ + iB_2^+\right\}\right], \tag{31}$$

where B_1^+ represents the equivalent elastic solution given by Yamakawa (1962):

$$B_1^+ = \frac{\xi_+^3}{3}\left(1 - \frac{\rho'}{\rho}\right), \tag{32}$$

where ρ and ρ' represent overall densities of background and inclusion. The numerical analysis of the velocity dispersion in the full frequency range is carried out in the next section.

As stated before, our model is limited to small concentrations of inclusions δ. Note, that the velocity limits for low and high frequencies are known. For low frequencies the velocity is given by Berryman & Milton (1991) and for high frequencies by an effective elastic model with isolated elastic inclusions. It is, therefore, important to check that our model satisfies those limits. The problem is, however, that in general even these high- and low-frequency asymptotical velocities are not uniquely defined by the volume concentration of inclusions but depend on their spatial distributions. This makes the comparisons quite cumbersome. However, for the special case of patchy saturation the low- and high-frequency velocity are unique functions of volume concentrations and are given by Gassmann-Wood and Gassmann-Hill bounds, respectively. The Gassmann-Wood low-frequency bound on seismic velocity reads (Johnson 2001)

$$v_{\rm BGW} = \sqrt{\frac{H_{\rm BGW}}{\rho}}, \tag{33}$$

where $H_{\rm BGW}$ represents fluid-saturated bulk modulus given by Gassmann's eq. (5), where the fluid modulus M given by eq. (4) implements the effective pore fluid bulk modulus K_W using Wood formula

$$\frac{1}{K_W} = \frac{1-\delta}{K_f} + \frac{\delta}{K_f'}. \tag{34}$$

The high-frequency velocity $v_{\rm BGH}$ reads (Johnson 2001):

$$v_{\rm BGH} = \sqrt{\frac{K_{\rm BGH} + 4\mu/3}{\rho}}, \tag{35}$$

and $K_{\rm BGH}$ represents the fluid-saturated bulk modulus given by Hill's theorem

$$\frac{1}{K_{\rm BGH} + 4\mu/3} = \frac{1-\delta}{K + 4\mu/3} + \frac{\delta}{K' + 4\mu/3}, \tag{36}$$

where K, K' are fluid-saturated bulk moduli of background and inclusion media given by Gassmann's eq. (1). For this case eq. (31) reduces to

$$\frac{1}{v_{\rm eff}} = \frac{1}{v_+}\left[1 + \frac{3}{2}\frac{\delta}{\xi_+^3}\mathrm{Re}\left\{-iB_0^+ + B_1^+\right\}\right]. \tag{37}$$

Since our model is limited to small concentrations of inclusions, this velocity is not identical to the one given by Gassmann-Wood bound. However, in the limit of low concentrations of inclusions the expression (37) in power of δ gives

$$\frac{v_{\rm eff}}{v_{\rm BGW}} = 1 + O(\delta^2). \tag{38}$$

Since the higher order term in low-frequency limit scales with δ, we conclude that our model is asymptotically consistent with Gassmann's theory for small concentration of inclusions.

In the limit of high frequency, the effective velocity $v_{\rm eff}$ fulfil the no-flow limit given by Gassmann-Hill bound (eq. 36) on seismic velocity $v_{\rm BGH}$ and the expression (37) in power of δ gives:

$$\frac{v_{\rm eff}}{v_{\rm BGH}} = 1 + O(\delta^2). \tag{39}$$

The more general case, for which the bounds are uniquely determined by δ, is the case of effective elastic moduli of an elastic composite with dilute concentration of elastic spheres (Christensen 1979). For this model effective elastic constants are given by

$$\frac{\mu_e^*}{\mu_e} = 1 - \frac{15(1-\nu_e)\left[1 - \left(\frac{\mu'}{\mu_e'}\right)\right]\delta}{7 - 5\nu_e + 2(4-5\nu_e)\left(\frac{\mu_e'}{\mu_e}\right)}, \tag{40}$$

$$K_e^* = K_e + \frac{(K_e' - K_e)\delta}{1 + \left[(K_e' - K_e)/\left(K_e + \frac{4}{3}\mu\right)\right]}, \tag{41}$$

where $\nu_e = (3K_e - 2\mu_e)/2(3K_e + \mu_e)$ represents Poisson's ratio. Using these results and combining them with Gassmann's equation allow constructing general lower and upper bounds on the porous material with the porous inclusions of another material. The only limitations

Table 1. Mechanical properties of the sample rocks.

Parameter	Background	Inclusion 1	Inclusion 2
K_0 [GPa]	12.6×10^9	11.97×10^9	12.6×10^7
μ_0 [GPa]	9.0×10^9	8.55×10^9	9.0×10^7
κ [m^2]	0.95×10^{-12}	0.95×10^{-12}	0.95×10^{-12}
ϕ	0.16	0.16	0.16
K_g [GPa]	33×10^9	33×10^9	33×10^9
ρ_g [kg m^3]	2760	2760	2760

are saturating fluid and grain material which are the same in both background medium and inclusion. Under these conditions the lower bound (low-frequency limit) on seismic velocity yields

$$v^*_{Lf} = \sqrt{\frac{K^*_{Lf} + 4\mu^*_{Lf}/3}{\rho}}, \tag{42}$$

where K^*_{Lf} and μ^*_{Lf} are given by Gassmann's fluid substitution

$$K^*_{Lf} = K^*_0 + \sigma^{*2} M^*, \tag{43}$$

$$\mu^*_{Lf} = \mu^*_0, \tag{44}$$

and K^*_0 and μ^*_0 are obtained using eqs (41) and (40) by substituting dry bulk modulus of background and inclusion ($K_e = K_0, K'_e = K'_0$). The parameters σ^* and M^* are given by eqs (2) and (4) and read

$$\sigma^* = 1 - \frac{K^*_0}{K_g}, \tag{45}$$

$$\phi^* = \phi(1-\delta) + \phi'\delta, \tag{46}$$

$$M^{*-1} = \left[\frac{\sigma^* - \phi^*}{K_g} + \frac{\phi^*}{K_f}\right], \tag{47}$$

where K_g represents grain bulk modulus.

The upper bound (high-frequency limit) on seismic velocity v^*_{Hf} is constructed as follows:

$$v^*_{Hf} = \sqrt{\frac{K^*_{Hf} + 4\mu^*_{Hf}/3}{\rho}}, \tag{48}$$

where K^*_{Hf} and μ^*_{Hf} are obtained using eqs (41) and (40) by substituting fluid-saturated bulk modulus of background and inclusion ($K_e = K, K'_e = K'$).

To check that effective velocity in eq. (31) satisfies at low-and high-frequency generalized bounds given by eqs (42) and (48), we expand our results in powers of δ. In the low-frequency limit for small concentration of inclusions the effective velocity v_{eff} from eq. (31) gives

$$\frac{v_{\text{eff}}}{v^*_{Lf}} = 1 + O(\delta^2), \tag{49}$$

and in the limit of high frequencies the

$$\frac{v_{\text{eff}}}{v^*_{Hf}} = 1 + O(\delta^2). \tag{50}$$

The dispersion curves and their limiting cases are in the full frequency range investigated numerically in the following section.

3.3 Numerical examples

In Figs 2–6 and 7(a) we show the attenuation and dispersion in the broad frequency range We use in our examples sample rock parameters summarized in Table 1 and the parameters of water and gas (Table 2).

To check the correctness of the expressions (23) and (24) in Fig. 2, we compare the derived analytical model with the numerical solution for the scattering by single inclusion. The porous background medium and the inclusion were in both cases saturated with water. The two types of models were tested. The lower attenuation curve (in Fig. 2) represents the comparison for the case of low contrast between elastic

Table 2. Mechanical properties of fluids.

Parameter	Water	Gas
K_f [GPa]	2.25×10^9	0.0001×10^9
ρ_f [kg m^3]	1000	1.2
η [Pa s]	0.001	0.000018

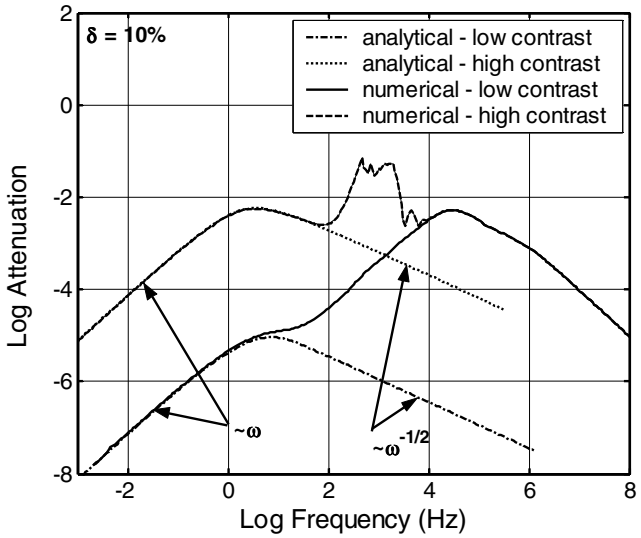

Figure 2. Comparison of the derived analytical solution (eq. 23) of *P*-wave attenuation with the general numerical solution.

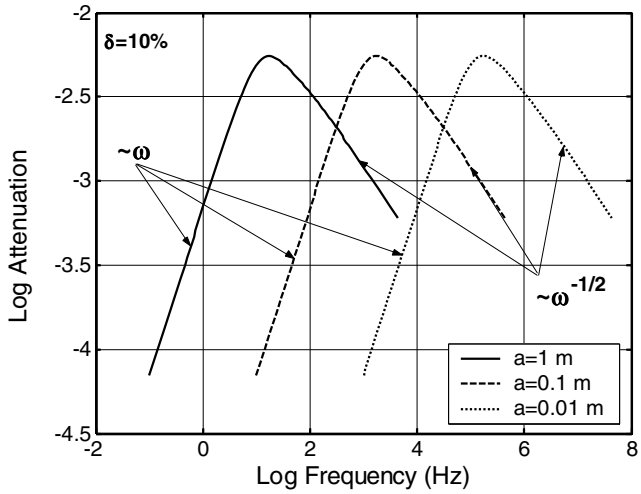

Figure 3. Effective attenuation due to scattering into the Biot's slow wave versus frequency for inclusions of different size. Attenuation maximum shifts to higher frequencies as the inclusion radius *a* decreases.

constants of background medium and inclusion (Table 1, Inclusion 1). The upper attenuation curve represents the case when the contrast between background and inclusion is high (Table 1, Inclusion 2). This comparison shows very good agreement between our model and the numerical solution up to a certain frequency. Beyond this frequency the numerical solution deviates substantially from the analytical solution. This occurs due to other attenuation mechanisms, namely elastic (Rayleigh) scattering and Biot's visco-inertial mechanism, both of which dominate at high frequencies that violate the low-frequency assumptions stated in Section 2.1 (Fig. 2). The frequency dependence of the attenuation has a form of a relaxation peak, with the maximum of the dimensionless attenuation at a frequency at which the wavelength of the Biot's slow wave is approximately equal to the characteristic size of the inclusion. This figure confirms the asymptotical behaviour derived in the previous section.

Fig. 3 shows the attenuation curves for the special case of patchy saturation (eq. 24). The uniform porous background with parameters given in Table 1 saturated with air (Table 2) contains randomly distributed spherical patches of water (Table 2). The asymptotical behaviour derived still holds. The attenuation maximum shifts to higher frequencies as the inclusion radius decreases. The same situation is analysed in Fig. 4 for effective velocity dispersion (eq. 37). The dispersion curves shift to higher frequencies with the decreasing radius of inclusions. The dispersion fits the bounds on seismic velocity given by eqs (38) and (39).

The behaviour of effective attenuation as a function of changing permeability in the inclusion's properties is shown in Fig. 5. The attenuation maximum keeps the same height and shifts to higher frequencies with increasing permeability. Fig. 6 shows the increase in the attenuation due to the increasing number of randomly distributed inclusions in the background medium. Maximum attenuation is growing but in this case it is fixed to constant frequency.

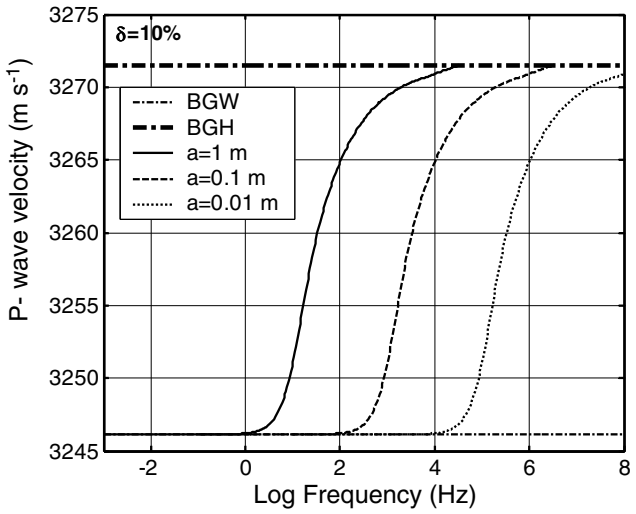

Figure 4. Effective velocity dispersion due to scattering into the Biot's slow wave versus frequency for inclusions of different size. Dispersion curves shift to higher frequencies as the inclusion radius *a* decreases.

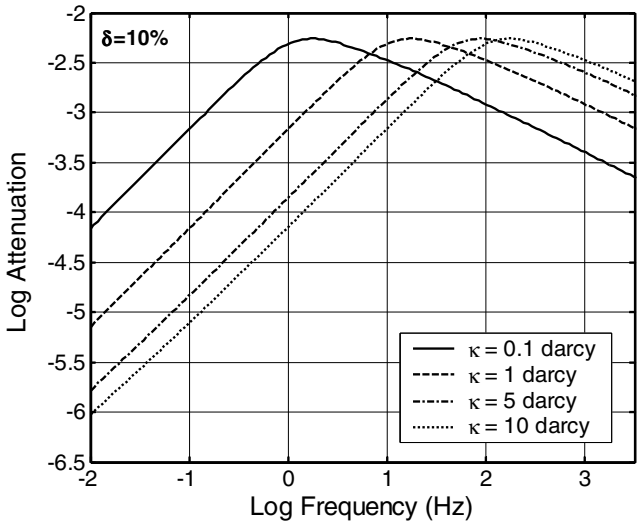

Figure 5. Effective attenuation versus frequency for different permeabilities of inclusions.

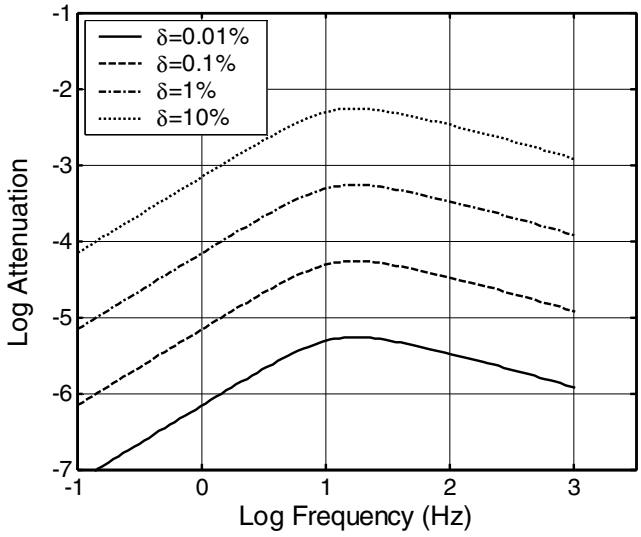

Figure 6. Effective attenuation versus frequency for different inclusion concentrations.

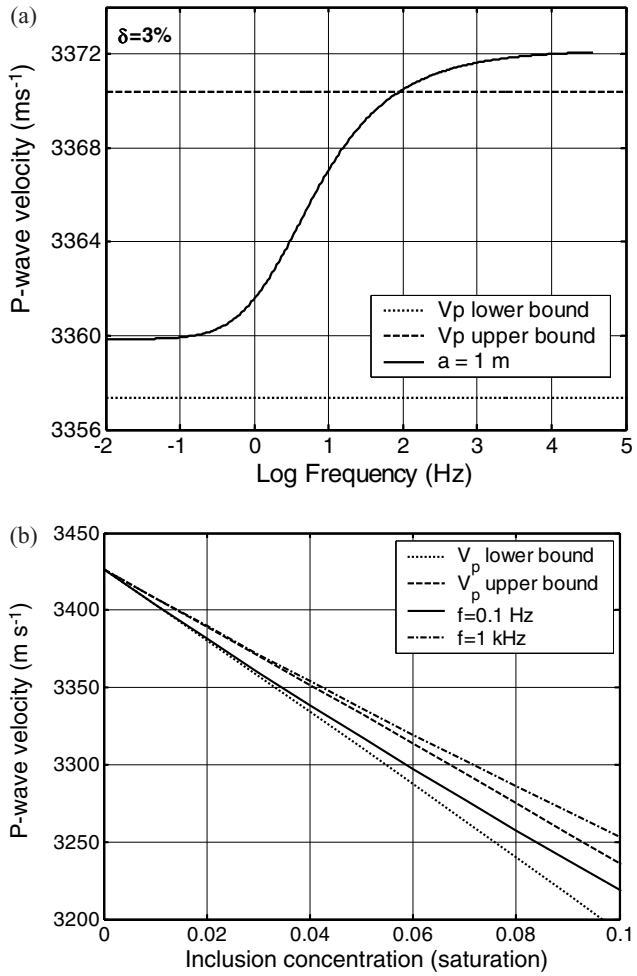

Figure 7. (a) Effective velocity dispersion versus frequency in the model of high contrast between inclusion and background parameters (Table 1, inclusion 1). Dispersion curve overestimates the generalized high- and low-frequency bounds for the inclusion concentration $\delta = 3$ per cent. (b) Effective *P*-wave velocity versus inclusion concentration. Dispersion curve fits the bounds at concentration 1 per cent and less.

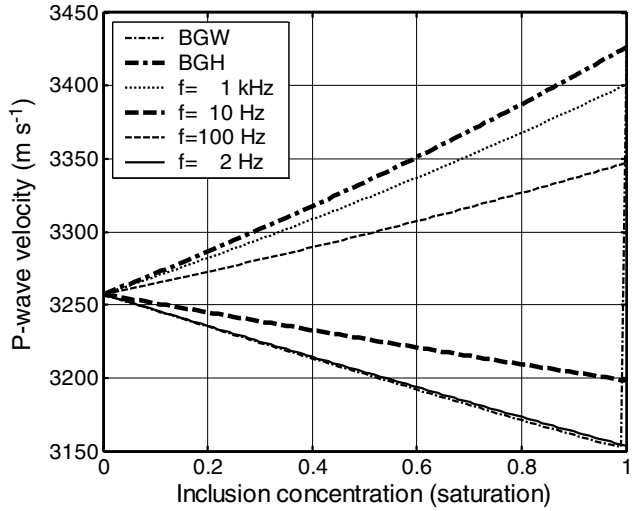

Figure 8. Effective *P*-wave velocity versus saturation in a model of spherical fluid patches. In this special case of patchy saturation this model fits the bounds on effective velocities up to 90 per cent of inclusion concentration.

The developed model for effective attenuation and velocity dispersion is limited to low concentration of inclusions. Fig. 8 shows that in some special cases (the case of patchy saturation) this model fits the bounds on effective velocities up to 90 per cent of inclusion concentration. This figure demonstrates the capability of the model to simulate frequency dependent behaviour of effective velocity due to increasing concentration of water patches. The limitation given by the assumption of low concentration of inclusions is shown in Fig. 7(a). The dispersion curve is shifted to higher effective velocities and overestimates the bounds even though the concentration is relatively low ($\delta = 3$ per cent). The violation of the limit in Fig. 7(a) is due to the high contrast between the fluid properties of the host and inclusion [water vs. air, see Table 1, Inclusion 1)]. We have deliberately chosen this case to highlight the limitations of the model. The effect has the same cause as very sharp drop of acoustic velocity with the addition of a only a few per cent of air into a liquid (or a liquid-saturated porous medium).

To show that the high- and low-frequency limits discussed in eqs (42) and (48) are satisfied at low concentrations we plot in Fig. 7(b) the effective velocity as a function of inclusion concentration. This figure confirms the theoretical analysis. At concentrations as low as 1 per cent the effective velocity fits the high- and low-frequency bounds.

These numerical examples demonstrate the behaviour of the derived model of randomly distributed poroelastic spherical inclusions in a poroelastic background medium in full frequency range and confirm the analytically derived limiting cases.

4 CONCLUSIONS

The main result of this study is the quantitative model of scattering of elastic waves by spherical poroelastic inclusions randomly distributed in a poroelastic background medium. These inclusions cause attenuation and dispersion of the incident fast compressional wave due to mode conversion into Biot's slow wave. This mechanism concerns wave-induced flow caused by heterogeneity in the elastic moduli at 'mesoscopic' scales. The explicit formula derived in this study quantifies this attenuation mechanism. It needs to be pointed out that this expression is fully derived without fitting the limits unlike the models of Johnson (2001) and Pride & Berryman (2003).

The analysis of this mechanism reveals following conclusions. At low frequencies, the attenuation scales with frequency ω and at high frequencies is proportional to frequency as $\omega^{-1/2}$. Attenuation increases with the concentration of spherical inclusions. The increasing size of the inclusions causes shift in the position of the attenuation maximum to the lower frequencies. Attenuation maximum shifts to higher frequencies when the permeability of inclusions is growing. Dispersion curves are consistent with the results obtained for the attenuation and shift to higher frequencies when the size of inclusions decreases. In the case of patchy saturation the derived dispersion model satisfies the upper and lower limits expressed by Hill's and Wood's theorems. This model is consistent with the upper and lower bounds derived from the effective elastic moduli of elastic composite material containing dilute concentration of spherical inhomogeneities. The derived analytical model is in good agreement with the numerical solution.

The model with spherical inclusions is very idealized and is unlikely to explain observed levels of attenuation and dispersion in real rocks, except perhaps in the case of partially saturated rocks. However, the idealized model presented can be used to develop more advanced models for more complicated geometries.

ACKNOWLEDGMENTS

The work of RC was supported by CSIRO Postdoctoral Fellowship Program. The work of BG was supported by the Centre of Excellence for Exploration and Production Geophysics, CSIRO Division of Petroleum Resources and by Curtin Reservoir Geophysics Consortium.

REFERENCES

Abramowitz, M. & Stegun, I.A., 1965. *Handbook of Mathematical Functions*, Chap. 10, Dover, New York.

Berryman, J.G., 1985. Scattering by a spherical inhomogeneity in a fluid-saturated porous medium, *J. Math. Phys.,* **26**(6), 1408–1419.

Berryman, J.G. & Milton, W.M., 1991. Exact results for generalized Gassmann's equations in composite porous media with two constituents, *Geophysics,* **56,** 1950–1960.

Biot, M.A., 1962. Mechanics of deformation and acoustic propagation in porous media, *J. Appl. Phys.,* **33**(4), 1482–1498.

Christensen, R.M., 1979. *Mechanics of Composite Materials*, John Wiley & Sons.

Ciz, R. & Gurevich, B., 2005. Amplitude of Biot's slow wave scattered by a spherical inclusion in a fluid-saturated poroelastic medium, *Geophys. J. Int.,* **160,** 991–1005.

Deresiewicz, H. & Skalak, R., 1963. On uniqueness in dynamic poroelasticity, *Bull. Seis. Soc. Am.,* **53,** 409–416.

Dutta, N.C. & Ode, H.C., 1979a. Attenuation and dispersion of compressional waves in fluid-filled rocks with partial gas saturation (White Model)-Part I: Biot theory. *Geophysics,* **44,** 1777–1788.

Dutta, N.C. & Ode, H.C., 1979b. Attenuation and dispersion of compressional waves in fluid-filled porous rocks with partial gas saturation (White Model)-Part II: results. *Geophysics,* **44,** 1789–1805.

Gassmann, F., 1951. Elastic waves through a packing of spheres, *Geophysics,* **16,** 673–685.

Gubernatis, J.E., Domany, E. & Krumhansl, J.A., 1977. Formal aspects of the theory of the scattering of ultrasound by flaws in elastic materials, *J. Appl. Phys.,* **48,** 2804–2811.

Gurevich, B. & Lopatnikov, S.L., 1995. Velocity and attenuation of elastic waves in finely layered porous rocks, *Geophys. J. Int.,* **121,** 933–947.

Gurevich, B., Sadovnichaja, A.P., Lopatnikov, S.L. & Shapiro, S.A., 1998. Scattering of a compressional wave in a poroelastic medium by an ellipsoidal inclusion, *Geophys. J. Int.,* **133,** 91–103.

Johnson, D.L., 2001. Theory of frequency dependent acoustics in patchy-saturated porous media, *J. acoust. Soc. Am.,* **110**(2), 682–694.

Korneev, V.A. & Johnson, L.R., 1993a. Scattering of elastic waves by a spherical inclusion—I. Theory and numerical results, *Geophys. J. Int.,* **115,** 230–250.

Korneev, V.A. & Johnson, L.R., 1993b. Scattering of elastic waves by a spherical inclusion—I. Limitations of asymptotic solutions, *Geophys. J. Int.,* **115,** 251–263.

Krutin, V.N., Markov, M.G. & Yumatov, A.Y., 1984. Scattering of a longitudal wave by a spherical cavity with a fluid in an elastic porous medium, *Appl. Math. Mech.,* **48,** 333–336.

Lopatnikov, S.L. & Gurevich, B., 1986. Attenuation of elastic waves in a randomly inhomogeneous saturated porous medium, *Doklady Earth Science Sections,* **291**(6), 19–22.

Muller, T. & Gurevich, B., 2005. Wave-induced fluid flow in porous random media: attenuation and dispersion of seismic waves, *J. acoust. Soc. Am.,* **117**(5), 2732–2741.

Norris, A.N., 1993. Low-frequency dispersion and attenuation in partially saturated rocks, *J. acoust. Soc. Am.,* **94,** 359–370.

Pride, S.R. & Berryman, J.G., 2003. Linear dynamics of double-porosity double-permeability materials, I. Governing equations and acoustic attenuation, *Physical Review E,* **68**(3): 036603-1–036603-10.

Pride, S.R. *et al.*, 2003, Permeability dependence of seismic amplitudes, *The Leading Edge,* **22**(6), 518–525.

Pride, S.R., Berryman, J.G. & Harris, J.M., 2004. Seismic attenuation due to wave-induced flow, *J. geophys. Res.,* **109**(B1), B01201.

Waterman, P.C. & Truell, R., 1961. Multiple scattering of waves, *Journal of Mathematical Physics,* **2**(4), 512–537.

White, J.E., 1975. Computed seismic speeds and attenuation in rocks with partial gas saturation. *Geophysics,* **40,** 224–232.

White, J.E., Mikhaylova, N.G. & Lyakhovitskiy, F.M., 1976. Low-frequency seismic waves in fluid-saturated layered rocks, *Phys. Solid Earth, Trans. Izv.,* **11,** 654–659.

Yamakawa, N., 1962. Scattering and attenuation of elastic waves, *Geophys. Mag.* (Tokyo) **31,** 63–97.

Ying, C.F. & Truell, R., 1956. Scattering of a plane longitudinal wave by a spherical obstacle in an isotropically elastic solid, *J. Appl. Phys.,* **27,** 1086–1097.

Zimmerman, C. & Stern, M., 1993. Scattering of plane compressional waves by a spherical inclusion in a poroelastic medium, *J. acoust. Soc. Am.,* **94,** 527–536.